

A Unitarized Chiral Approach to $f_0(980)$ and $a_0(980)$ States and Nature of Light Scalar Resonances

Masayuki UEHARA*
Takagise-Nishi 2-10-17, Saga 840-0921, Japan

December 6, 2018

Abstract

We show that the $f_0(980)$ and $a_0(980)$ states appearing in scattering and production processes can be described quite well by the two-channel Oller-Oset-Peláez (OOP) version of unitarized chiral theories. It is impossible, however, to deduce a decisive conclusion on the nature of them from the fitting to experimental data alone. Using explicit N_c dependence of parameters in OOP amplitudes we demonstrate that light scalar resonances are not of $q\bar{q}$ states but dynamical rescattering effects generated under chiral symmetry, unitarity and channel couplings.

@@ @ @ @ @ @ @ @ @

1 Introduction

Probably we have not yet reached a consensus on the nature of light scalar mesons below 1 GeV[1, 2]. Main issues around them are whether they are real propagating particles or are dynamical rescattering effects, whether they are of $q\bar{q}$ states, four quark states or $K\bar{K}$ molecule states, and whether they form a nonet within themselves or only one or two are needed to form a different nonet with higher mass scalar states.

In order to study these issues many authors focus on the analyses of the $f_0(980)$ and $a_0(980)$ states appearing in decay processes such as $\phi \rightarrow \gamma f_0(980)$ and $\phi \rightarrow \gamma a_0(980)$. In most theoretical approaches the radiative ϕ decays take place through a radiative charged kaon loop diagram so as to satisfy the Okubo-Zweig-Iizuka (OZI) rule. The difference in various approaches comes from the way how to construct amplitudes $K^+K^- \rightarrow m_1 m_2$ including the $f_0(980)$ or $a_0(980)$ states, where m_1 and m_2 are final two pseudoscalar mesons. Among the ways we quote models using $f_0(980)$ and $a_0(980)$ propagators[3, 4, 5], unitarized chiral approaches[6, 7, 8, 9, 10], a model using the linear sigma model[11, 12], a compound model of chiral $O(p^2)$ terms and propagators[13], and a model with channel couplings between hadronic and quark channels[14]. There are approaches without using the explicit kaon-loop mechanism; a model in which production amplitudes are assumed to be proportional to scattering amplitudes with real coefficient functions in order to satisfy unitarity[15], and a quark model with a radiative quark loop by assuming that all these mesons are to be dominantly $q\bar{q}$ states[16]. Similarly, $\gamma\gamma \rightarrow f_0$ and a_0 processes are expected to reveal the quark structure of them[17]. How unambiguously can we determine both theoretical and experimental branching fraction $B(\phi \rightarrow \gamma f_0)$? Calculating a pole and its residues of the $f_0(980)$ state, Boglione and Pennington[15] have given $B(\phi \rightarrow \gamma f_0)$ much smaller than the usually quoted value $(3.4 \pm 0.4) \times 10^{-4}$ [18]. This indicates that we should be cautious of extracting the correct signal of the $f_0(980)$ state from experimental mass distributions. If this is the case, it becomes obscure whether we can reach a decisive conclusion on the nature of the $f_0(980)$ and $a_0(980)$ states through these analyses.

In this paper we attempt to describe the $f_0(980)$ and $a_0(980)$ states appearing in scattering and production processes within the two-channel Oller-Oset-Peláez version[19], that is an approximate version of Inverse Amplitude Method (IAM)[20, 21, 22, 23, 24] to unitarize amplitudes up to $O(p^4)$ of Chiral

*E-mail: ueharam@cc.saga-u.ac.jp

Perturbation Theory (ChPT)[25, 26]. The basic ingredients of $SU(3) \times SU(3)$ ChPT are the octet Nambu-Goldstone particles π , K , η_8 , where we treat η_8 as the physical η in the two-channel OOP version, and any scalar meson fields are not introduced as independent degrees of freedom in advance. It offers, therefore, a good theoretical framework to study the issues. Of course, this does not imply that the existence or non-existence of a resonance can be predicted by IAM, since ChPT amplitudes of $O(p^4)$ include a set of phenomenological parameters, low energy constants (LECs), which are to be determined so as to reproduce experimental data. After having fixed the LECs, the multi-channel amplitudes are determined without any additional free parameters. Though our set of the LECs are not the best solution, the phase shifts are reproduced quite well. Since two-meson mass spectra of the radiative ϕ meson decays depend on the off-diagonal $K^+K^- \rightarrow \pi\pi$ and $K^+K^- \rightarrow \pi\eta$ scattering amplitudes below the $K\bar{K}$ threshold, the resulting mass spectra offer a proving ground of the OOP amplitudes. It turns out that the mass spectra are reproduced fairly well by the OOP amplitudes. In $\gamma\gamma \rightarrow \pi\pi$ processes, however, the $f_0(980)$ signal is masked by complicated interferences, since various production mechanism contribute coherently. This process is a proving ground of production mechanisms, if we have more accurate data near the f_0 state, therefore.

Even if IAM or its OOP version can give simultaneous fits to scattering and production data, it is impossible to deduce a decisive conclusion on the quark structure of the $f_0(980)$ and $a_0(980)$ states because of the reason stated above on the LECs. We should note, however, that the pion decay constant f_π and the LECs in ChPT have a definite N_c dependence, where N_c is the number of colors. Due to this nature of the theory we can study how scalar amplitudes behave when N_c increases from 3. It has been shown recently that the scalar states do not survive as N_c is larger than 3, and then the scalar states are probably not $q\bar{q}$ states but dynamical ones, while vector mesons survive as narrow resonances as typical $q\bar{q}$ states[27, 28]. In this sense IAM and its approximate OOP version can give not only a unified description of scattering and production processes but also an insight into the quark structure of the light scalar mesons.

We discuss the OOP description of scattering processes in the next section, including a discussion on LECs used in this paper. Scalar meson productions in radiative ϕ meson decays and $\gamma\gamma$ collisions are discussed in Sec. 3, and the large N_c behavior of scalar states are discussed in Sec.4, and concluding remarks are given in the last section.

2 The OOP description of scattering processes

2.1 The OOP amplitude

The ingredients of IAM consist of chiral order $O(p^2)$ and $O(p^4)$ amplitudes of ChPT. An $O(p^2)$ amplitude, denoted by $T^{(2)}(s, t, u)$, has a form of a linear function of s , t , u and meson mass squared divided by f_π^2 , where s , t and u are the usual Mandelstam variables. An $O(p^4)$ amplitude is composed of polynomial terms and one-loop terms: A polynomial term, denoted by $T_{\text{poly}}^{(4)}(s, t, u)$, is given as a sum of quadratic functions of s , t , u and meson mass squared with the LECs, denoted as L_n , as follows:

$$T_{\text{poly}}^{(4)}(s, t, u) = \sum_{n=1,8} \frac{1}{f_\pi^4} L_n P_n(s, t, u), \quad (2.1)$$

where P_n are the quadratic functions. Loop terms are given by $T^{(2)} \times T^{(2)}$ with divergent loop integrals, which are regularized in the $\overline{MS} - 1$ scheme at the renormalization scale μ [25, 26]. An s -channel loop term is given by $t^{(2)}(s)J(s)t^{(2)}(s)$, where $t^{(2)}$ is a partial wave amplitude derived from $T^{(2)}(s, t, u)$ and $J(s)$ is the one-loop function which will be given soon. There are similar t - and u -channel loop terms and tadpole terms, but they are discarded in the OOP version. The ingredients of amplitudes in the OOP version consist of the $O(p^2)$ terms, the polynomial and the s -channel loop terms of $O(p^4)$ amplitudes. We use the $O(p^4)$ amplitudes given in Ref. [23], where the kaon and η decay constants are set equal to the pion decay constant f_π in order to guarantee exact perturbative unitarity.

The two-channel OOP amplitudes are written in the symmetric 2×2 matrix form as

$$\mathbf{T}(s) = \mathbf{t}^{(2)}(s)[\mathbf{t}^{(2)}(s) - \mathbf{t}^{(4)}(s)]^{-1} \mathbf{t}^{(2)}(s), \quad (2.2)$$

where $\mathbf{t}^{(2)}(\mathbf{t}^{(4)})$ is the 2×2 partial wave amplitude with chiral order $O(p^2)$ ($O(p^4)$) amplitude and s is the total center of mass (CM) energy squared. Our T-matrix is normalized as

$$S_{ij}(s) = \delta_{ij} - 2i\rho_i^{1/2}(s)T_{ij}(s)\rho_j^{1/2}(s), \quad (2.3)$$

$$\rho_i(s) = \frac{1}{16\pi}\frac{2k_i}{\sqrt{s}}\theta(s - s_i) \quad (2.4)$$

where ρ_i is the phase space factor with k_i (s_i) being the CM momentum (threshold energy squared) of the i -th channel. The partial wave $\mathbf{t}^{(4)}(s)$ is given as

$$\mathbf{t}^{(4)}(s) = \mathbf{t}_{\text{poly}}^{(4)}(s) + \mathbf{t}^{(2)}(s) \cdot \mathbf{J}(s) \cdot \mathbf{t}^{(2)}(s), \quad (2.5)$$

where $\mathbf{t}_{\text{poly}}^{(4)}(s)$ is the partial waves of $T_{\text{poly}}^{(4)}(s, t, u)$, and $\mathbf{J}(s)$ is the diagonal 2×2 loop integral; $J_i(s)$ of the i -th channel is written

$$\begin{aligned} J_i(s) &= \frac{1}{(4\pi)^2} \left\{ -1 + \log\left(\frac{m_1 m_2}{\mu^2}\right) + \frac{\Delta_{21}}{s} \log\left(\frac{m_2}{m_1}\right) \right. \\ &\quad \left. + \lambda_i(s) \log\left(\frac{\sigma_{i+}(s) + \sigma_{i-}(s)}{\sigma_{i+}(s) - \sigma_{i-}(s)}\right) \right\}, \end{aligned} \quad (2.6)$$

$$\sigma_{i\pm} = \sqrt{1 - (m_1 \pm m_2)^2/s}, \quad (2.7)$$

$$\lambda_i(s) = \sigma_{i+}(s)\sigma_{i-}(s) \quad (2.8)$$

for the channel with unequal masses m_1 and m_2 in the i -th channel, and $\Delta_{21} = m_2^2 - m_1^2$. Because the imaginary part of $J_i(s)$ is given as

$$\text{Im}J_i(s) = -\rho_i(s), \quad (2.9)$$

$\mathbf{T}(s)$ satisfies the exact s -channel unitarity relation

$$\text{Im}T_{ij}(s) = -T_{ik}^*(s)\rho_k(s)T_{kj}(s). \quad (2.10)$$

The LECs, L_1 to L_8 , are determined so as to reproduce S -wave $\pi\pi$ phase shifts up to about 1.2 GeV. It should be noted that our fitting covers a wide energy range from the $\pi\pi$ threshold to 1 GeV or more including resonances, that the LECs appear in \mathbf{T} non-linearly and that the OOP version discards the t - and u -channel loop terms and tadpole terms of the full $O(p^4)$ amplitudes. So that our set of the LECs and μ could be different from those of ChPT determined through low energy data below the lowest resonance region. The scale μ has a meaning corresponding to a cut-off parameter as discussed in Ref. [19], and we set $\mu = 0.87$ GeV, that is larger than usually adopted value $\mu = m_\rho$ by about 100 MeV. Our set of the LECs are given as

$$\begin{aligned} L_1 &= 0.70 \times 10^{-3}, & L_2 &= 1.30 \times 10^{-3}, & L_3 &= -3.20 \times 10^{-3}, \\ L_5 &= 1.50 \times 10^{-3}, & L_7 &= -0.25 \times 10^{-3}, & L_8 &= 0.71 \times 10^{-3}, \end{aligned} \quad (2.11)$$

and L_4 and L_6 are fixed equal to zero.

2.2 The $(\mathbf{I}, \mathbf{J}) = (0, 0)$ channel: $\pi\pi \times K\bar{K}$

The characteristic behavior of this channel is that the $\pi\pi$ phase shift δ_{11}^{00} rises from the $\pi\pi$ threshold, forms a plateau of $50^\circ \sim 80^\circ$ from 500 to 800 MeV, crosses 90° in the region $800 \sim 900$ MeV, and suddenly increases over 200° just below the $K\bar{K}$ threshold. This feature is reproduced quite well as shown in Fig. 1 (a). The phase shift calculated in the single $\pi\pi$ channel formalism cannot exceed 90° as shown by the dotted line in Fig. 1 (a). On the other hand a bound state pole appears in the $K\bar{K}$ channel, when the channel coupling to the $\pi\pi$ channel is switched off. A weak coupling to the $\pi\pi$ channel generates a narrow resonance behavior in the $\pi\pi$ channel. The steep rising of the $\pi\pi$ phase shift near the $K\bar{K}$ threshold is due to the interference between the $\pi\pi$ background and the narrow resonance born as the $K\bar{K}$ bound state. In this sense the $f_0(980)$ state is called a bound state resonance[29, 30, 31, 32, 33]. Also shown are the production rate defined by $(1 - \eta_{00}^2)/4$ with η_{00} being the inelasticity and the the

phase, $\delta_{12}^{00} = \delta_{11}^{00} + \delta_{22}^{00}$, above the $K\bar{K}$ threshold. These give the size and the phase of the off-diagonal scattering amplitude T_{12} above the $K\bar{K}$ threshold.

In our set of the LECs and μ the phase shift δ_{11}^{00} crosses 90° at 875 MeV. The scattering lengths are given as

$$a_{00} = 0.217 \text{ } m_\pi^{-1} \quad a_{20} = -0.041 \text{ } m_\pi^{-1}. \quad (2.12)$$

According to Ref. [42] ChPT up to two loop accuracy gives

$$a_{00} = 0.220 \pm 0.005 \quad a_{20} = -0.0444 \pm 0.0010. \quad (2.13)$$

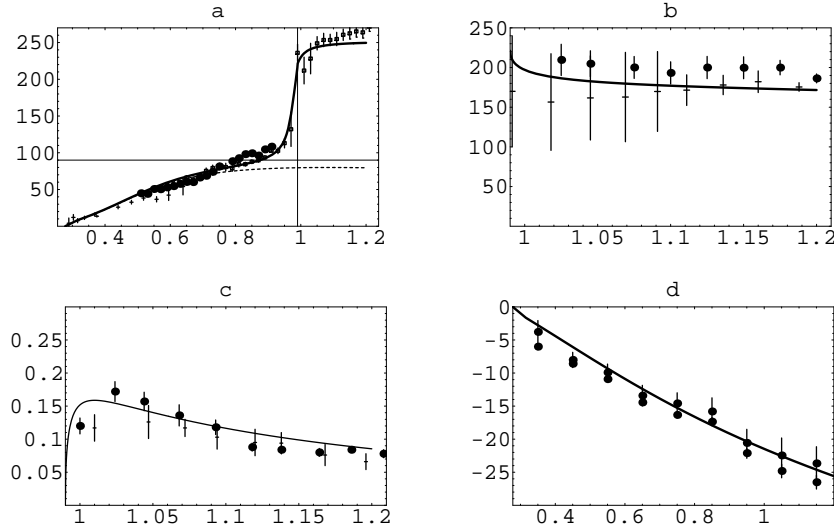


Figure 1: (a) The $\pi\pi$ phase shift δ_{11}^{00} . The solid (dotted) line represents the result of the two- (single $\pi\pi$ -)channel calculation. The vertical (horizontal) line represents the $K\bar{K}$ threshold (90°). Experimental data are full circles [34], blank squares [35], bars [36, 37], and triangles [38]. (b) $\pi\pi \rightarrow K\bar{K}$ phase, δ_{12}^{00} . Experimental data are taken from [39]. (c) $(1 - \eta_{00}^2)/4$. The data are full circles [39] and bars [40]. (d) δ^{20} with the data from [41]. The abscissas are the invariant $\pi\pi$ mass in units of GeV.

The phase difference $\delta^{(00)} - \delta^{(20)}$ at the kaon mass is 49.9° , which is the phase of two-pion decay amplitudes of a kaon originating from the final state interactions. Recently the KLOE collaboration gives $(48 \pm 3)^\circ$ [43], and ChPT does $(47.7 \pm 1.5)^\circ$ [42].

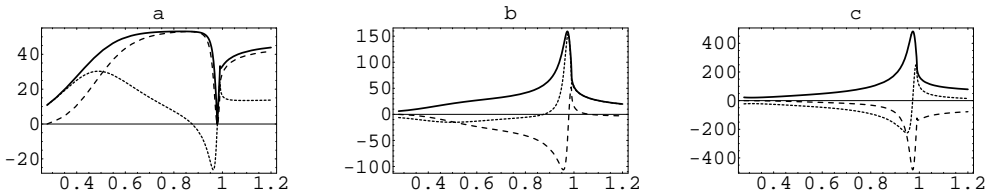


Figure 2: Energy dependence of $-T_{ij}$. (a) $-T_{11}$. (b) $-T_{12}$. (c) $-T_{22}$. The solid lines are the absolute values, the dotted lines the real parts, and the dashed lines the imaginary parts.

We also show all of the amplitudes T_{ij} in Fig. 2. The f_0 structure appears as a sharp dip in T_{11} owing to the interference with the large background, which is often called the $\sigma(600)$ state, but T_{12} and

T_{22} show the clear peak corresponding to the f_0 state just below the $K\bar{K}$ threshold. The magnitude and shape of T_{12} below the $K\bar{K}$ threshold is crucial to the $\phi \rightarrow \gamma\pi\pi$ decays, and it turns out that our OOP amplitude T_{12} reproduces the $\pi\pi$ mass spectra fairly well.

2.3 The $(I, J) = (1, 0)$ channel: $\pi\eta \times K\bar{K}$

Since there are almost no experimental data on extrapolated $\pi\eta$ elastic scattering, the $\pi\eta$ mass distributions from $K^-p \rightarrow \pi^-\eta\Sigma^+(1385)$ reaction[44] and $pp \rightarrow p(\eta\pi^+\pi^-)p$ reaction[45] have been compared with theoretical works[23, 19, 32, 46]. The former reaction is expected to give data of the $K\bar{K} \rightarrow \pi\eta$ process, and the latter to derive information on the elastic $\pi\eta \rightarrow \pi\eta$ process, but the data is not sufficient. We do not give the phase shift and cross section here, therefore. (These are shown in Sec.4.)

The $(K\bar{K})_{I=1}$ scattering amplitude in the single channel formalism has a bound state, but the situation is much different from the f_0 case; the bound state disappears when the $\pi\eta$ coupling is switched off, and the $\pi\eta$ elastic channel is repulsive in the single channel formalism. The channel coupling between the $\pi\eta$ and $K\bar{K}$ channels is strong in this channel, however, and then the production rate $(1 - \eta_{(10)}^2)/4$ reaches almost the maximum value 0.25. This strong channel coupling generates the a_0 structure as pointed out in the meson-exchange model[31] and unitarized chiral theories[32, 33]. Thus, the generating mechanism of $a_0(980)$ is different from that of $f_0(980)$; the channel coupling is crucial for both, but it is strong for the former but weak for the latter.

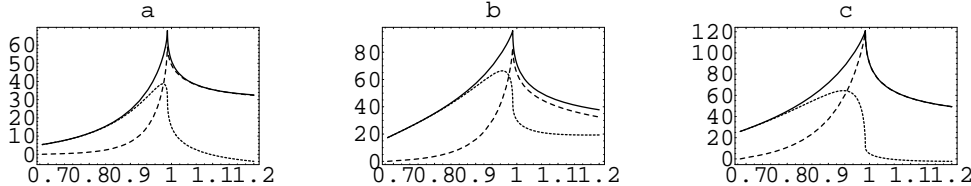


Figure 3: Energy dependence of $-T_{ij}$. (a) $-T_{11}$. (b) $-T_{12}$. (c) $-T_{22}$. The lines are the same as in Fig.2.

The amplitudes T_{ij} in the $(1, 0)$ channel show the common shape having a sharp cusp-like peak at the $K\bar{K}$ threshold as shown in Fig. 3. This feature will be examined in the $\pi\eta$ mass spectra observed in radiative reactions $\phi \rightarrow \pi\eta$ and $\gamma\gamma \rightarrow \pi\eta$.

2.4 Other partial waves

The $(I, J) = (1/2, 0)$ and $(3/2)$ phase shifts are described qualitatively well by our OOP amplitudes, though the results are not shown. But better fitting is obtained if we use $f_K = 1.22f_\pi$. The scattering lengths are

$$a_{1/2,0} = 0.216 \quad (0.161) \quad a_{3/2,0} = -0.054 \quad (-0.049) \quad (2.14)$$

in units of (m_π^{-1}) , where the values in the parentheses are for the case that $f_K = 1.22f_\pi$, while ChPT gives [47]

$$a_{1/2,0} = 0.17 \pm 0.02 \quad a_{3/2,0} = -0.05 \pm 0.02. \quad (2.15)$$

The vector resonances, ρ and $K^*(890)$, are also reproduced well by our OOP amplitudes. The mass and width of the ρ meson are 784 MeV and 162 MeV, respectively. Those of the K^* meson are 818 MeV and 28 MeV, respectively, for $f_K = f_\pi$. In the case that $f_K = 1.22f_\pi$ the obtained values are 900 MeV and 45 MeV, respectively.

Thus, we say that the validity of the two-channel OOP amplitudes is confirmed.

2.5 Pole search for the f_0 and a_0 states

The OOP amplitudes T_{ij} can be decomposed into a pole term and its background term as

$$T_{ij}(s) = \Gamma_i(s)\Delta(s)\Gamma_j(s) + U_{ij}(s), \quad (2.16)$$

where $\Gamma_i(s)$ is the one-particle irreducible form factor of the i -th channel, $\Delta(s)$ is the propagator of the relevant particle, and U_{ij} is the background amplitude satisfying unitarity by themselves[48]. The form factor Γ_i satisfies the unitarity relation,

$$\text{Im}\Gamma_i(s) = -U_{ij}^*(s)\rho_j(s)\Gamma_j(s), \quad (2.17)$$

and then the phase of Γ_i is controlled by those of U_{ij} .

The propagator $\Delta(s)$ continued to the second Riemann sheet has a complex conjugate pair of poles, and the pole near the real axis on the lower half-plane contributes to the physical amplitude as

$$P_{ij} = g_i e^{i\alpha_i} \left[\frac{1}{s - W_R^2} \right] g_j e^{i\alpha_j}, \quad (2.18)$$

where $g_i e^{\alpha_i}$ is the form factor $\Gamma_i(s)$ at $s = M_R^2$, and $W_R = M_R - iM_I$ with M_R (M_I) being the real (imaginary) part of the pole. The poles and residues are tabulated in Table 1.

$f_0(980)$		$a_0(980)$	
$W_R = (978.4 - 19.7i)$ MeV		$W_R = (1110.4 - 8.9i)$ MeV	
$g_1 = 1.54$ (GeV)	$g_2 = 4.57$ GeV	$g_1 = 6.63$ GeV	$g_2 = 8.50$ GeV
$\alpha_1 = -85.6^\circ$	$\alpha_2 = -15.8^\circ$	$\alpha_1 = -8.5^\circ$	$\alpha_2 = -36.1^\circ$

Table 1: Pole positions, residues and phases of the $f_0(980)$ and $a_0(980)$ states.

It should be noticed that the pole of the a_0 state appears above the $K\bar{K}$ threshold by 120 MeV, while the pole of the f_0 state exists below the threshold and the distance between the two poles is about 130 MeV. Nevertheless all the amplitudes T_{ij} of the isovector channel show the cusp-like behavior at the $K\bar{K}$ threshold, and then the two peaks appear very close to each other in physical processes. The large phase α_1 for the f_0 pole indicates a large contribution from the background of the $\pi\pi \rightarrow \pi\pi$ amplitude, that is due to the σ enhancement centered at 500 MeV. On the other hand α_1 for the a_0 pole is small, and then $\pi\eta \rightarrow \pi\eta$ scattering may be dominated by the pole term, but the size of α_2 indicate that background contribution is not ignored.

We quote examples of the poles and their residues of previous works:

$$\begin{aligned} f_0 & W_R = (0.987 - 0.011i) \text{ GeV} & (g_1, g_2) = (1.18, 3.83) \text{ GeV}, \\ a_0 & W_R = (1.030 - 0.086i) \text{ GeV} & (g_1, g_2) = (4.08, 5.60) \text{ GeV} \end{aligned} \quad (2.19)$$

in the two-channel calculation[49], and

$$f_0 \quad W_R = (0.989 - 0.022i) \text{ GeV} \quad (g_1, g_2) = (1.155, 1.227) \text{ GeV} \quad (2.20)$$

in [15], where g_2 is much smaller than that of Eq.(2.19) and our value in Table 2.

If we define the partial width as an integral[15],

$$\Gamma_i = \frac{2M_I}{\pi} \int_{s_i}^{\infty} ds \frac{\rho_i(s)g_i^2}{|W_R^2 - s|^2}, \quad (2.21)$$

we have

$$\Gamma_{\pi\pi} = 45.3 \text{ MeV} \quad \Gamma_{K\bar{K}} = 39.4 \text{ MeV} \quad (2.22)$$

for the $f_0(980)$ state, and the sum of the partial widths, 77.8 MeV, is larger than $2M_I = 35.4$ MeV by a factor 2. As to the $a_0(980)$ state the same definition gives huge partial widths;

$$\Gamma_{\pi\eta} = 567 \text{ MeV} \quad \Gamma_{K\bar{K}} = 554 \text{ MeV} \quad (2.23)$$

because of the large residues. Such huge partial widths have already been pointed out by Flatté[50], who shows that the partial $\pi\eta$ width could be 300 MeV, when the Flatté phase space factor $\rho_F(s)$ is used, where $\rho_F(s) = \rho_2(s)$ for $s > s_2$, and $\rho_F(s) = i|\rho_2(s)|$ for $s < s_2$. These facts cast doubt not only on the above definition of the partial widths but also the conventional resonance interpretation of a_0 in contrast to an isolated narrow resonance.

In order to extract the pole contribution from the whole amplitudes, we have to express the pole term $P_{ij}(s)$ in a region away from the pole position. After testing the Breit-Wigner form, the Flatté form and the loop form used in Ref. [4], we find that the Breit-Wigner form is suitable to the f_0 state, where we compare the Breit-Wigner amplitudes

$$P_{ij}(s) = \frac{g_i g_j}{s - M_R^2 + i M_R(\rho_1 g_1^2 + \rho_2 g_2^2)} \quad (2.24)$$

with the T_{ij} amplitude; we observe that the two 12 amplitudes resemble with each other near the f_0 resonance peak, except for the phase because of neglecting the phase $\alpha_{12} \sim 90^\circ$ in P_{12} . See Fig. 4.

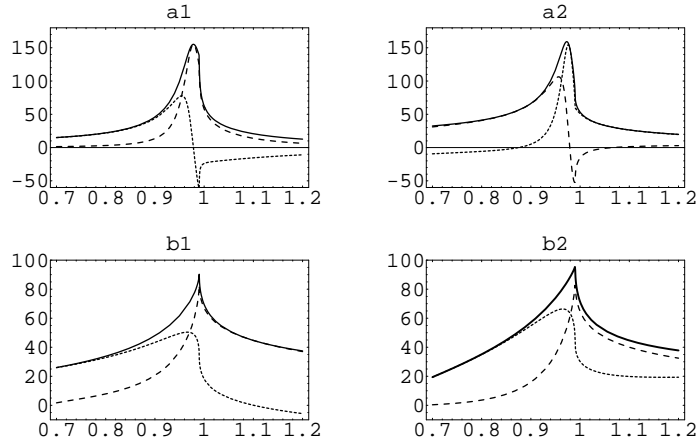


Figure 4: (a) The f_0 state. The left side is $-P_{12}$ and the right side $+ReT_{12}$, $-ImT_{12}$. (b) The a_0 state. The left side is $-P_{12}$ and the right side is $-T_{12}$. The solid lines are the absolute values, the dotted lines the real parts and the dashed lines the imaginary parts. Note that the real and imaginary parts are exchanged between the left and right side of (a) because of $\alpha_1 + \alpha_2 \sim -90^\circ$.

But it turns out that in order to reproduce the sharp cusp-like behavior in the isovector channel the Flatté form is required, where ρ_F is used instead of ρ_2 , as shown in Fig. 4 (b). The loop form is useful to the f_0 state, but not for a_0 state, because the depression of the real part is insufficient below the $K\bar{K}$ threshold. The residues strongly depress scattering amplitudes below the $K\bar{K}$ threshold in the Flatté form.

Another method to extract the pure f_0 amplitude is to assume the form of U_{ij} as a single channel elastic amplitude as

$$U_{ij}(s) = \frac{[t_{11}^{(2)}(s)]^2}{t_{11}^{(2)}(s) - t_{11}^{(4)}(s) - J_1(s)[t_{11}^{(2)}(s)]^2} \delta_{i1} \delta_{j1}, \quad (2.25)$$

and subtract it from T_{11} . The extracted f_0 amplitude is given as [51]

$$f_0(s) = (T_{11}(s) - U_{11}(s))e^{-2i\delta_U(s)} \quad (2.26)$$

where δ_U is the phase shift of U_{11} . From this definition the mass and the width of the f_0 state are

$$M_{f_0} = 977.7 \text{ MeV} \quad \Gamma_{f_0} = 35.6 \text{ MeV}, \quad (2.27)$$

where M_{f_0} is defined as a mass at which the phase shift of $f_0(s)$ crosses 90° , and

$$\Gamma_{f_0}^{-1} = \frac{1}{2} \frac{d\delta_{f_0}(s)}{d\sqrt{s}}|_{\sqrt{s}=M_{f_0}}. \quad (2.28)$$

The values in Eq.(2.27) are very close to the pole position in Table 1. In this case there are no background term in $\pi\pi \rightarrow K\bar{K}$ and $K\bar{K} \rightarrow K\bar{K}$ amplitudes, and T_{12} and T_{22} are dominated by the f_0 state alone. Indeed, the clear peak structure appears both in these amplitudes, but it would not be true that there are no background term in these amplitudes.

3 The f_0 and a_0 states in production processes

3.1 Radiative ϕ meson decays

Many theoretical calculations of the radiative ϕ meson decays are based on the common production mechanism, in which the final S-wave two-meson scattering amplitude is connected to the initial decay vertex through the charged kaon loop. The validity of the on-shell factorizability of the loop and the scattering amplitudes is discussed in Refs. [32, 6, 7, 52].

According to Ref.[7] we write the decay amplitude of the ϕ meson to two-meson state $\gamma m_1 m_2$ as

$$F(\phi \rightarrow \gamma m_1 m_2) = 2eg\{G_K(s) + f \frac{m_\phi^2 - s}{2m_\phi^2} J_K(s)\} T_{K^+ K^- \rightarrow m_1 m_2}, \quad (3.1)$$

where $m_1 m_2$ means $\pi^0 \pi^0$, $\pi^0 \eta$ or $K^0 \bar{K}^0$, and g and f are the parameters defined as

$$g = \frac{G_V m_\phi}{\sqrt{2} f_\pi^2} \quad \text{and} \quad f = \frac{F_V}{2G_V} - 1 \quad (3.2)$$

with G_V and F_V being the constants in the chiral Lagrangian[53, 54, 7] and a factor $1/\sqrt{2}$ in g is the ratio of the coupling constant $\rho\pi\pi$ to $\phi K\bar{K}$. The triangle $K\bar{K}$ loop integral $G_K(s)$, which connects the ϕ meson to the S-wave two-meson state after emitting a photon, is given as [3, 55, 5]

$$G_K(s) = \frac{1}{(4\pi)^2} \left\{ 1 + \frac{m_k^2}{s - m_\phi^2} \left[\log^2 \left(\frac{\sigma_K(s) + 1}{\sigma_K(s) - 1} \right) - \log^2 \left(\frac{\sigma_K(m_\phi^2) + 1}{\sigma_K(m_\phi^2) - 1} \right) \right] \right. \\ \left. - \frac{m_\phi^2}{s - m_\phi^2} \left[\sigma_K(s) \log \left(\frac{\sigma_K(s) + 1}{\sigma_K(s) - 1} \right) - \sigma_K(m_\phi^2) \log \left(\frac{\sigma_K(m_\phi^2) + 1}{\sigma_K(m_\phi^2) - 1} \right) \right] \right\}, \quad (3.3)$$

and $J_K(s)$ is the kaon two-point loop function given in Eq.(2.6). The scattering amplitude $T_{K^+ K^- \rightarrow m_1 m_2}$ is $T_{K^+ K^- \rightarrow \pi\pi}$ or $T_{K^+ K^- \rightarrow \pi\eta}$, which is obtained in the previous section. We adopt the values $G_V = 55$ MeV and $F_V = 165$ MeV given in [7], which are suited to the $\phi \rightarrow K^+ K^-$ and $\phi \rightarrow e^+ e^-$ decay widths, respectively, and then we have $g = 4.69$ and $f = 0.5$. We emphasize that there are left no adjustable parameters, and then the mass spectra are a proving ground of the validity of $T_{12}(s)$ below the $K\bar{K}$ threshold.

The mass dependence of the two-meson state in the radiative decay is given as

$$\frac{d\Gamma(s)}{d\sqrt{s}} = \left(\frac{\alpha}{3\pi} \right) \left(\frac{g^2}{4\pi} \right) \frac{k_f(m_\phi^2 - s)}{m_\phi^3} \left| \tilde{F}(\phi \rightarrow \gamma m_1 m_2) \right|^2, \quad (3.4)$$

where k_f is the momentum of a final meson in the rest frame of the final $(m_1 m_2)$ state, and we define \tilde{F} as $F = 2eg\tilde{F}$. The s -dependence of the phase space factor $k_f(m_\phi^2 - s)/m_\phi^3$ has the maximum near the middle of the whole \sqrt{s} -range, and vanishes at both ends. Furthermore, the loop integral $G_K(s) + f(m_\phi^2 - s)/(2m_\phi^2) \cdot J_K(s)$ has a strong cusp behavior at the $K\bar{K}$ threshold, which is very near to m_ϕ , so that the mass distributions near 1 GeV are affected double by these kinematical factors.

The calculated mass distributions of the $\phi \rightarrow \gamma\pi^0\pi^0$ and $\phi \rightarrow \gamma\pi^0\eta$ decays reproduce the experimental data fairly well except for the mass region from 400 to 650 MeV of the $\phi \rightarrow \gamma\pi\pi$ decay, where the mass

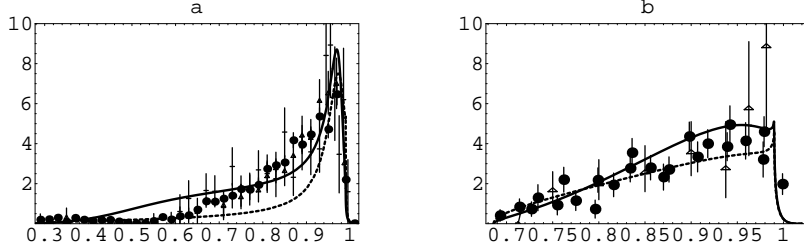


Figure 5: (a) $dB(\phi \rightarrow \pi^0\pi^0)/d\sqrt{s} \times 10^4/\text{GeV}$. The solid line is the result of the full amplitude and the dotted one that of the pole-terms. Experimental data are taken from [56, 57, 58]. (b) $dB(\phi \rightarrow \gamma\pi^0\eta)/d\sqrt{s} \times 10^4/\text{GeV}$. The lines are the same as in (a). Experimental data are taken from [59, 60].

distribution shows a shallow dip. See Fig. 5. Our results strongly indicate the validity of both of our scattering amplitudes and the production mechanism. The calculated and experimental branching fractions are tabulated in Table 2 and 3, respectively. The $\pi\pi$ mass distribution below 700 MeV for $\phi \rightarrow \gamma\pi^0\pi^0$ is affected by dominant backgrounds $\omega\pi^0 \rightarrow \gamma\pi^0\pi^0$ and $\rho\pi^0 \rightarrow \gamma\pi^0\pi^0$ as stressed in [56, 57]. It is better, therefore, to compare a theoretical calculation with experimental date above 700 MeV.

	$B(\phi \rightarrow \gamma\pi^0\pi^0)$	$B(\phi \rightarrow \gamma\pi^0\eta)$
Whole mass range	1.29×10^{-4}	0.875×10^{-4}
$w > 700 \text{ MeV}$	0.917×10^{-4}	
$w > 900 \text{ MeV}$	0.493×10^{-4}	
Pole contribution	0.655×10^{-4}	0.701×10^{-4}

Table 2: Branching fractions integrated over the indicated mass ranges.

$B(\phi \rightarrow \gamma\pi^0\pi^0) \cdot 10^4$	CMD-2	SND	KLOE
whole mass range	$1.08 \pm 0.17 \pm 0.09$	$1.158 \pm 0.093 \pm 0.052$	$1.09 \pm 0.03 \pm 0.05$
$w > 700 \text{ MeV}$	$0.92 \pm 0.08 \pm 0.06$	$1.034 \pm 0.066 \pm 0.046$	$0.96 \pm 0.02 \pm 0.04$
$w > 900 \text{ MeV}$	$0.57 \pm 0.06 \pm 0.04$	$0.559 \pm 0.053 \pm 0.025$	
$B(\phi \rightarrow \gamma\pi^0\eta) \cdot 10^4$	CMD-2	SND	KLOE
whole mass range	$0.90 \pm 0.24 \pm 0.10$	$0.88 \pm 0.14 \pm 0.09$	$0.851 \pm 0.051 \pm 0.057^*$

Table 3: Experimental data on the branching fractions, where CMD-2 is referred to [56], SND to [57, 59] and KLOE to [58, 60]. * means the data in which η is identified through $\eta \rightarrow \gamma\gamma$, and it becomes $(0.796 \pm 0.060 \pm 0.040)$ when $\eta \rightarrow 3\pi$ decay is used.

Our results $B(\phi \rightarrow \gamma\pi^0\pi^0) = 0.917 \times 10^{-4}$ above 700 MeV and $B(\phi \rightarrow \gamma\pi^0\eta) = 0.875 \times 10^{-4}$ are consistent with the data in Table 3. The problem is what parts of the mass distributions can be attributed to the contributions from "pure" $f_0(980)$ and $a_0(980)$ states. If we use the pole terms, the usual Breit-Wigner form for f_0 and the Flatté form for a_0 given the previous section, we have $B(\phi \rightarrow \gamma f_0 \rightarrow \gamma\pi\pi) = (0.655 \times 3 = 1.965) \times 10^{-4}$ and $B(\phi \rightarrow \gamma a_0 \rightarrow \gamma\pi\eta) = 0.701 \times 10^{-4}$, both of which are the values integrated over the whole mass range. The f_0 pole contribution above 900 MeV is 0.413×10^{-4} , that is 84 % of the $\pi^0\pi^0$ distribution in the same mass range, and $B(\phi \rightarrow \gamma a_0 \rightarrow \gamma\pi\eta) = 0.701 \times 10^{-4}$ is 80 % of the whole $\pi\eta$ mass distribution. The pole contribution dominates the mass distributions above 900 MeV for the $\gamma\pi^0\pi^0$ decay, while the pole contribution dominates the whole mass distribution for

the $\gamma\pi^0\eta$ decay. Here we note that these values can be regarded as the branching fractions of the whole $B(\phi \rightarrow \gamma f_0)$ and $B(\phi \rightarrow \gamma a_0)$, because the $K\bar{K}$ contributions are negligibly small due to the small phase space.

Finally we obtain

$$B(\phi \rightarrow \gamma K^0 \bar{K}^0) = 4.26 \times 10^{-8} \quad (3.5)$$

for the neutral kaon pair decay. In order to get this value the mass difference between the neutral and charged kaon plays an important role to suppress the phase space; we use 497.67 MeV for K^0 here, while 495 MeV is used for the kaon mass throughout this paper. Our result is very similar to the values of previous works; 4.36×10^{-8} in the second paper of [4] and 5.0×10^{-8} in [6]. The charged kaon pair production is dominated by the Born terms including the Bremsstrahlung terms, and then it is almost irrelevant to the f_0 and a_0 states.

3.2 Two-photon collision processes

Two-photon collision processes are not so suitable to study the f_0 states in contrast to the radiative ϕ meson decays, because the charged kaon loop dominance does not hold. The Born terms with the charged pion exchange and ω -meson exchange contribute to $\pi^+\pi^-$ and $\pi^0\pi^0$ production, respectively, and the charged pion loop and $\omega\pi^0\pi^0$ loop diagrams contribute to these production processes. And there are contributions from higher partial waves and the phase space are opened. Indeed, experimental $\pi\pi$ mass distributions seem not to show manifest signals of the f_0 state[61, 62, 63]. On the other hand the a_0 production seems not to be worried with various production mechanisms besides the charged kaon triangle loop diagram as in the radiative ϕ meson decay. We discard the $\omega\gamma\eta$ and $\rho\gamma\pi$ vertices, because their coupling constants are much smaller than that of the $\omega\gamma\pi^0$ vertex. Focusing on the S -wave pion pair and $\pi^0\eta$ production processes we study $\gamma\gamma \rightarrow m_1 m_2$ processes through the charged pion and kaon loop diagrams and the ω exchange diagrams, which are developed in Refs.[64, 65, 66].

The production amplitude $F_f(w)$ from the initial photon state with the helicity $(++)$ to the final S -wave $m_1 m_2$ state f can be written

$$F_f(s) = -2e^2 \left(B_f(s) + \sum_{i=1,3} T_{fi}(s) G_i(s) \right), \quad (3.6)$$

where the final state f denotes charged pion pair, neutral pion pair and $\pi^0\eta$ states, and the intermediate state $i = 1$ means the charged pair, $i = 2$ the charged kaon pair state, and $i = 3$ the $\pi^0\pi^0$ state generated in the $\omega\pi^0\pi^0$ triangle loop. $B_f(s)$ is the Born term, but $B_{\pi\eta} = 0$, and T_{fi} is the $i \rightarrow f$ scattering amplitude. The triangle loop functions $G_1(w)$ and $G_2(s)$ are the integrals of the charged pion and kaon loop diagram, respectively, which is given as

$$G_i(s) = \frac{1}{(4\pi)^2} \left\{ 1 + \frac{m_i^2}{s} \log^2 \left(\frac{\sigma_i(s) + 1}{\sigma_i(s) - 1} \right) \right\}. \quad (3.7)$$

The loop function G_3 with the ω exchange without any form factor is given in Ref.[64], which is rewritten in Appendix because of a lengthy expression. The discontinuity of $G_i(s)$ across the physical cut gives the Born term as

$$\text{Im}G_i(s) = -\rho_i(s)B_i(s) = -\rho_i(s) \left[\frac{2m_i^2}{s\sigma_i(s)} \log \left(\frac{1 + \sigma_i(s)}{1 - \sigma_i(s)} \right) \right] \quad (3.8)$$

for $i = 1$ and 2, and

$$\text{Im}G_3(s) = -\rho_1(s)B_3(s) = -\rho_1(s) \cdot \frac{-R_\omega}{\sqrt{2}} \left\{ -s + \frac{M_\omega^2}{\sigma_1(s)} \log \left(\frac{1 + v(s) + \sigma_1(s)}{1 + v(s) - \sigma_1(s)} \right) \right\}, \quad (3.9)$$

where B_3 is the ω exchange Born term with $R_\omega = 1.35 \text{ GeV}^{-2}$ [65], $v(s) = 2(M_\omega^2 - m_\pi^2)/s$, and a factor $1/\sqrt{2}$ is related to the definition of the cross section. The production amplitude F_f satisfies the final interaction theorem as

$$\text{Im}F_f(s) = - \sum_i T_{fi}^*(s) \rho_i(s) F_i(s),. \quad (3.10)$$

The S-wave two-meson production cross section of the f state is written as

$$\sigma_S^f(s) = 2\pi\alpha^2 \frac{\sigma_f(s)}{s} \left| \tilde{F}_f(s) \right|^2 \quad (3.11)$$

with $F_f = -2e^2 \tilde{F}_f$, and k_f is the CM momentum.

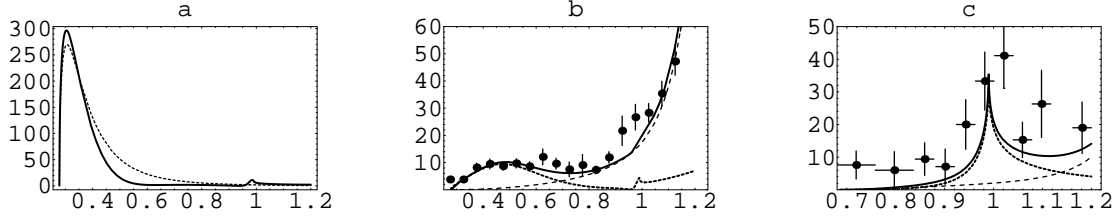


Figure 6: (a) $\gamma\gamma \rightarrow \pi^+\pi^-$ cross section integrated over $|\cos\theta| \leq 0.6$. The solid line is the total S -wave cross section, and the dashed one the Born term. The behavior near the f_0 region is given in the inner box. (b) $\gamma\gamma \rightarrow \pi^0\pi^0$ cross section integrated over $|\cos\theta| \leq 0.8$. The solid line shows the sum of the S -wave cross section and the $f_2(1280)$ resonance. The dotted line shows the S -wave cross section and the dashed one the $f_2(1280)$ cross section. The experimental data are taken from [61]. (c) $\gamma\gamma \rightarrow \pi^0\eta$ cross section integrated over $|\cos\theta| < 0.9$ with the $a_2(1320)$ resonance. The lines are the same as in (b). The experimental data are taken from [68, 69]

The calculated S -wave $\pi^+\pi^-$ cross section integrated over the region $|\cos\theta| < 0.6$ shows a large peak resulting from the Born term and a small f_0 signal coming from the rescattering terms as shown in Fig. 6 (a). The cross section integrated over the full angle is merely 18.6 nb/GeV at the f_0 peak. This is due to destructive interferences among the Born term and various rescattering terms. The small f_0 signal in the charged pion distribution appears to be consistent with the experimental mass distributions, which show no clear f_0 signal [62, 63]. The calculated S -wave $\pi^0\pi^0$ cross section integrated over the region $|\cos\theta| < 0.8$ shows a dip and a cusp, but not the f_0 signal. If we discard both the ω exchange Born term and the rescattering term with the $\omega\pi\pi$ loop, we can see a clear f_0 peak. This implies that the present form of the ω exchange amplitudes without any form factor strongly reduces the f_0 signal. We should remember, here, that the T_{11} amplitude does not show a peak but a sharp dip in the f_0 region, and that the rescattering terms with the charged pion loop and the $\omega\pi\pi$ loop contain the very T_{11} amplitude. The broad bump around 500 Mev comes mainly from the pion loop diagram with T_{11} . Our neutral pion mass distribution seems not to be inconsistent with the experimental mass distribution, but there may be some deficiencies in the region of f_0 state. We think, however, that these possible deficiencies do not imply the invalidity of the OOP amplitudes, but suggest the inadequacy of the treatment of production mechanisms.

As to the $\pi^0\eta$ production channel the sharp peak appears in our calculation, but the consistency with the experimental data is not clear. It is noted that we take into account the rescattering term with the charged kaon loop alone in order to calculate the $\pi^0\eta$ mass distribution. If there contribute other production mechanisms, the similar shape of the scattering amplitudes would not destroy the sharp peak structure. As stressed in Ref. [66] the axial vector meson exchange would enhance the peak.

The partial widths of the $f_0(980) \rightarrow \gamma\gamma$ and $a_0(980) \rightarrow \gamma\gamma$ have been expected to play a role to distinguish the structure of them as in the radiative ϕ decays [17]. We have learned in the above that different production mechanisms and their interference mask the f_0 signal in the charged and neutral pion pair production. We should be cautious, therefore, of the way how to estimate the partial $f_0\gamma\gamma$ width.

Taking the narrow width limit of the relativistic Breit-Wigner formula given in [61, 62], we can define the partial width by integrating the mass spectrum around the peak region as

$$\Gamma_{\gamma\gamma}(R \rightarrow f) = \frac{M_R}{8\pi^2} \int_{s_1}^{s_2} ds \sigma_{\gamma\gamma \rightarrow f}(s), \quad (3.12)$$

where $\sqrt{s_1}$ ($\sqrt{s_2}$) is 0.9 (1.05) GeV for f_0 and 0.8 (1.2) GeV for a_0 . The integration range is chosen so as reflect the form of the mass spectra. We obtain

$$\Gamma_{\gamma\gamma}(f_0 \rightarrow \pi^+\pi^-) = 0.056 \text{ keV}, \quad (3.13)$$

but we cannot estimate $\Gamma^{\gamma\gamma}(f_0 \rightarrow \pi^0\pi^0)$, because there is no f_0 signal. If we use the pole terms, $P_{ij}(s)$, written by the Breit-Wigner forms instead of T_{ij} , we observe peaks in both spectra deformed by the cusp behavior, and we obtain

$$\begin{aligned} \Gamma_{\gamma\gamma}(f_0 \rightarrow \pi^+\pi^-) &= 0.081 \text{ keV}, \\ \Gamma_{\gamma\gamma}(f_0 \rightarrow \pi^0\pi^0) &= 0.035 \text{ keV}. \end{aligned} \quad (3.14)$$

The sum is 0.116 keV, and we have

$$\Gamma_{\gamma\gamma}(f_0 \rightarrow \text{all}) = 0.20 \text{ keV}, \quad (3.15)$$

if we use $B(f_0 \rightarrow \pi\pi) = 0.58$ calculated from the partial widths Eq.(2.22).

Though the $\pi\eta$ spectrum cannot be expressed by the Breit-Wigner form, we use the same equation with the peak at the $K\bar{K}$ threshold, 990 MeV, and obtain

$$\Gamma_{\gamma\gamma}(a_0 \rightarrow \pi\eta) = 0.17 \text{ keV}. \quad (3.16)$$

If we use $(-\text{Im}T_{22} \cdot |G_2(s)|^2)$ instead of $(\rho_1(s)|T_{12}G_2(s)|^2)$ in order to estimate the total photo-partial width[66, 8], where T_{22} is $T_{K^+K^- \rightarrow K^+K^-}$ and T_{12} is $T_{K^+K^- \rightarrow \pi^0\eta}$, we obtain a value,

$$\Gamma_{\gamma\gamma}(a_0 \rightarrow \text{all}) = 0.27 \text{ keV}. \quad (3.17)$$

Due to the similarity of the pole terms to the full amplitudes, the photo-partial widths are almost unchanged.

Preceding theoretical estimates are

$$f_0(980) \quad \begin{cases} \Gamma_{\gamma\gamma}(f_0 \rightarrow \text{all}) = 0.20 \text{ keV} & [66], \\ \Gamma_{\gamma\gamma}(f_0 \rightarrow \text{all}) = 0.28_{-0.13}^{+0.09} \text{ keV} & [67]. \end{cases} \quad (3.18)$$

$$a_0(980) \quad \begin{cases} \Gamma_{\gamma\gamma}(a_0 \rightarrow \text{all}) = 0.27 \text{ keV} & [17], \\ \Gamma_{\gamma\gamma}(a_0 \rightarrow \text{all}) = 0.78 \text{ keV} & [66]. \end{cases} \quad (3.19)$$

The experimental data using the Breit-Wigner fits are summarized as follows:

$$f_0(980) \quad \begin{cases} \Gamma_{\gamma\gamma}(f_0 \rightarrow \text{all}) = 0.29 \pm 0.07 \pm 0.12 \text{ keV} & [62], \\ \Gamma_{\gamma\gamma}(f_0 \rightarrow \text{all}) = 0.31 \pm 0.17 \text{ keV} & [61], \end{cases} \quad (3.20)$$

$$a_0(980) \quad \begin{cases} \Gamma_{\gamma\gamma}(a_0 \rightarrow \pi\eta) = 0.19_{-0.10}^{+0.12} \text{ keV} & [68], \\ \Gamma^{\gamma\gamma}(a_0 \rightarrow \pi\eta) = 0.28 \pm 0.04 \pm 0.10 \text{ keV} & [69], \\ \Gamma_{\gamma\gamma}(a_0 \rightarrow \pi\eta) = 0.24 \pm 0.08 \text{ keV} & [70]. \end{cases} \quad (3.21)$$

In the above $\Gamma_{\gamma\gamma}(f_0 \rightarrow \text{all})$ of [62] and [61] are obtained from $\pi^+\pi^-$ and $\pi^0\pi^0$ spectrum, respectively, using the conventional isospin factor and the old PDG value of $B(f_0 \rightarrow \pi\pi) = 0.78$ [71]. It is dubious, however, to use a conventional isospin factor to estimate the full $\pi\pi$ decay width, because complicated interferences should probably mask the f_0 signal. As to the a_0 signal our value 0.17 keV is not inconsistent with the value 0.19 keV of [68], but is a little bit smaller than the average value[70].

Finally we briefly comment on J/ψ decays. The decays $J/\psi \rightarrow (\phi \text{ or } \omega)(\pi\pi)$ and $J/\psi \rightarrow \rho(\pi\eta)$ are also expected to specify the quark contents of the f_0 and a_0 states[72]. The two-pion mass spectrum of the former decay accompanied by ϕ shows a clear peak at the $K\bar{K}$ threshold as like as in $\phi \rightarrow \gamma(\pi\pi)$ [73]. This strongly suggests that the decay proceeds mainly through the kaon loop so as to make $T_{K\bar{K} \rightarrow \pi\pi}$ work effectively. On the other hand the mass spectrum of the two-pion decay with ω shows a large broad peak centered at about 450 MeV and a dip-bump structure near the $K\bar{K}$ threshold[74], that resembles to the $\gamma\gamma \rightarrow \pi^+\pi^-$ process. The f_0 signal seems to be masked. Indeed, the mass spectrum calculated in terms of the Born term, that is a direct S -wave $\pi\pi$ production term, the pion and kaon loop terms and a sequential decay mode $b_1(1240)\pi \rightarrow \omega\pi\pi$ gives the broad peak originated from the Born term and a

dip-cusp structure instead of the f_0 peak[75].¹ Further higher spin meson exchange diagrams would not be discarded.

The $J/\psi \rightarrow \rho(\pi\eta)$ decay would also include some decay mechanisms similar to the $J/\psi \rightarrow \omega(\pi\pi)$ decay, but the a_0 signal might not be masked so much as contrasted with the f_0 case, since the isovector scattering amplitudes have similar shape and do not have large backgrounds.

4 Large N_c behavior of scalar scattering amplitudes

In the previous two sections we have found that the OOP version of unitarized chiral theories can reproduce not only scattering but also production processes fairly well. It is not clear, however, what this success tells us about the so-called quark contents of the $f_0(980)$ and $a_0(980)$ states, because the OOP amplitudes contain phenomenological constants, which should be determined so as to be suited to the experimental data.

It is said that ChPT is an effective theory of low energy QCD[76, 25], and $q\bar{q}$ meson states become weakly interacting narrow resonances in the large N_c limit of QCD[77, 78]. It offers a useful means to reveal the the quark contents, therefore, to examine whether the scalar mesons survive as narrow resonances when N_c increases from the physical value $N_c = 3$. (See Ref. [28] for details.)

Because the pion decay constant f_π is of $O(N_c^{1/2})$ and the LECs, L_1, L_2, L_3, L_5 and L_8 are to be of $O(N_c)$, but $2L_1 - L_2, L_4, L_6$ and L_7 are of $O(1)$ [26, 79, 80, 81], we put

$$L_n(N_c) = \widehat{L}_n \cdot \frac{N_c}{3} + \Delta L_n, \quad (4.1)$$

$$f_\pi^2(N_c) = \widehat{f}_\pi^2 \cdot \frac{N_c}{3}, \quad (4.2)$$

where \widehat{L}_n satisfy the relations, $2\widehat{L}_1 - \widehat{L}_2 = \widehat{L}_4 = \widehat{L}_6 = \widehat{L}_7 = 0$, and ΔL_n are of $O(1)$. Thus, we have

$$\frac{L_n}{f_\pi^2} = \frac{\widehat{L}_n}{\widehat{f}_\pi^2} + \frac{\Delta L_n}{\widehat{f}_\pi^2} \cdot \frac{3}{N_c} \quad (4.3)$$

with $\widehat{f}_\pi = 93$ MeV. In the case of our LECs ΔL_n are given as

$$\Delta L_2 \times 10^3 = -0.10, \text{ and } \Delta L_7 \times 10^3 = -0.25, \quad (4.4)$$

and others are zero. The $T^{(2)}(s, t, u)$ is of $O(N_c^{-1})$ and $T_{\text{poly}}^{(4)}(s, t, u)$ is also of $O(N_c^{-1})$, because L_n/f_π^2 scales as $O(N_c^0)$ as seen in Eq.(4.3). The s -channel loop term given by $t^{(2)}(s)J(s)t^{(2)}(s)$ is of $O(N_c^{-2})$. This difference of the N_c dependence produces different behavior of the amplitudes when N_c becomes large. The change of the renormalization scale affects values of ΔL_n , but we do not consider the scale change explicitly because the ΔL_n terms fade out as N_c increases.

At first, we discuss the behavior of the ρ meson in the single channel calculation. The mass of the ρ meson is given as a zero of a sum of the term $[t^{(2)} - t_{\text{poly}}^{(4)}]$ of $O(N_c^{-1})$ and the real part of the loop contribution of $O(N_c^{-2})$. Since the mass is controlled by a combination of the LECs $(2L_1 - L_2 + L_3)$ of the former term [20], the mass stays almost constant for $N_c \geq 3$. Because the imaginary part of the loop term contributes to the width, the width decreases as $O(N_c^{-1})$. Thus, the ρ meson remains as narrower resonance almost at the same point as N_c increases as shown in Fig. 7. Other vector mesons such as $K^*(890)$ behave as the same as the ρ meson. If we extend the calculation to the two-channel OOP version, the results do not change. Thus, we can conclude that the vector mesons described by the OOP version behave as narrow resonances, and then have the nature consistent with the $q\bar{q}$ mesons.

As to the scalar mesons the situation is drastically changed. The N_c dependence of the phase shift and the cross section of the $(I, J) = (0, 0)$ channel are shown in Fig. 8, where N_c increases from 3 to 12.

¹Recalculation with the present set of the LECs also shows a dip with a rather small cusp.

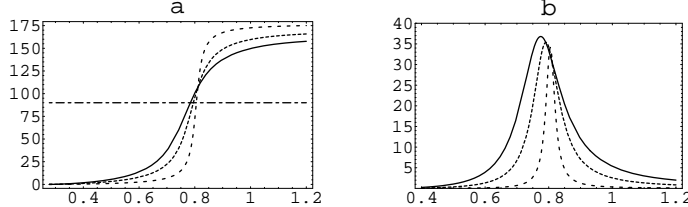


Figure 7: N_c dependence of phase shift (left) and cross section (right) of the ρ channel. Lines correspond to $N_c = 3, 5$ and 15 from the top to the bottom.

In contrast to the vector channel we observe that the phase shift becomes flat and the cross section fades out as N_c becomes large; the sharp rise of the phase shift near the $K\bar{K}$ threshold and the large bump of the cross section near 500 MeV seen at $N_c = 3$ to 5 disappears even at $N_c = 6$, and then the phase shift and the cross section become almost flat and fade out. Similar drastic change in the N_c dependence has also been observed in Ref. [82], though it is in quite different context.

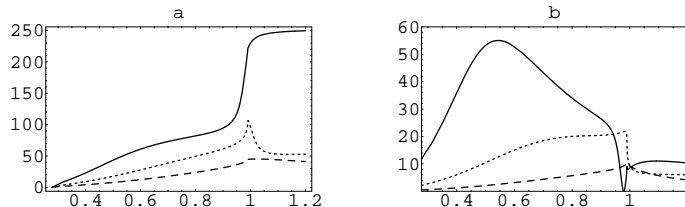


Figure 8: N_c dependence of the phase shift (left) and the cross section (right) of the $(0,0)$ channel. Solid, dotted, and dashed lines correspond to $N_c = 3, 6$ and 12 cases, respectively.

The $(I, J) = (1, 0)$ channel contains the $a_0(980)$ state and appears as a cusp-like sharp peak at $N_c = 3$ as seen in Fig. 9. The rising phase shift after the cusp bends down and becomes to a flat curve, and the cross section having a sharp peak fades out as N_c increases. The $(I, J) = (1/2, 0)$ channel show the same behavior as $(0, 0)$ and $(1, 0)$ channels.

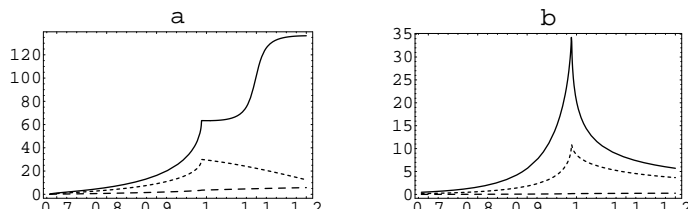


Figure 9: N_c dependence of the phase shift (left) and the cross section (right) of the $(1,0)$ channel. $N_c = 3, 4$ and 12 from the top to bottom.

We have shown in Sec. 3 that the $f_0(980)$ pole exists at $(978.4 - 19.7 i)$ MeV and the a_0 pole at $(1110.4 - 8.9 i)$ MeV at $N_c = 3$. Where do the poles go away as N_c increases? We make an approximate calculation of the pole positions by expanding the amplitudes in powers of k_2 up to the first order, where k_2 is the momentum of the $K\bar{K}$ channel. We observe that the poles move into the upper half plane of the IV sheet from the lower half plane of the II sheet, winding around the branch point at the $K\bar{K}$ threshold, and go away from the real axis as shown in Fig. 10. This approximation gives $W_{f_0} = (977.9 - 18.5 i)$ MeV

and $W_{a_0} = (1095.7 + 2.7 i)$ GeV at $N_c = 3$, which are close to the above values. Pole positions at larger N_c cannot be reliable owing to the rough approximation, but this behavior would remain unchanged.

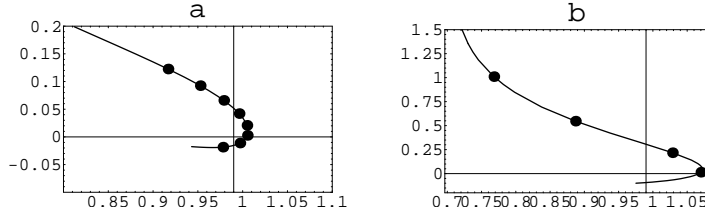


Figure 10: N_c dependence of the $f_0(980)$ pole (left) and $a_0(980)$ pole (right). Both of the poles wind around the branch point at $K\bar{K}$ threshold to go upward on the IV sheet. Black point starts at $N_c = 3$ and increases by 1 to 10 for f_0 and to 6 for a_0 .

We have calculated the N_c dependence of the vector and scalar channels starting from $N_c = 3$ to finite values, 30 for the vector channels and 15 for the scalar channels within the two-channel OOP version, and we have observed that the vector mesons survive as narrower resonances at almost the same position, but the resonant structures of the scalar channels fade out at rather low values of N_c near 5 or 6. By extending these observations we are led to a conclusion that the light vector meson nonet has the nature consistent with the $q\bar{q}$ mesons in large N_c QCD, but the light scalar meson nonet cannot survive in large N_c and then cannot have the nature of the $q\bar{q}$ mesons. This conclusion is the same as obtained by Peláez, excluding an exceptional case of the $a_0(980)$ state[27], where the full $O(p^4)$ amplitudes are used. It is also consistent with the result that the scalar mesons are describable without pre-existing tree resonance poles and then of dynamical origin, possibly except for $f_0(980)$ [46, 49]. If one treats the f_0 state within the two-channel model, the pre-existing resonance pole is not needed[49]. Our conclusion supports the arguments that the light scalar mesons are of the $K\bar{K}$ molecule[29, 30, 31], and of $q^2\bar{q}^2$ states[83, 84, 85, 3, 4, 5]. It is interesting to see that the lattice QCD calculation suggests that the masses of scalar mesons with $I = 0$ and $1/2$ are almost twice of those of the ρ and $K^*(890)$ mesons, respectively, if they are composed of connected $q\bar{q}$ lines[86].

5 Concluding remarks

In this paper we have discussed S -wave scattering processes and radiative production processes of two-pseudoscalar mesons in a unified manner. The scattering amplitudes are constructed within the two-channel OOP version and satisfy exact s -channel unitarity. We emphasize that the results of the radiative ϕ meson decays are the prediction by the two-channel OOP scattering amplitudes, once the decays occur dominantly through the charged kaon loop.

We have found that the scattering data are reproduced rather well, though we do not attempt to get the best parameter set. Radiative production processes reveal the structure of the transition amplitudes T_{12} below the $K\bar{K}$ threshold. Our results of the radiative ϕ meson decays show the validity of our amplitudes under the dominance of the $K\bar{K}$ loop mechanism as discussed in Sec. 3.1, where the $\pi^0\pi^0$ and $\pi^0\eta$ mass distributions are reproduced fairly well, at least above 700 MeV for the former channel, and then the branching fraction $B(\phi \rightarrow \gamma\pi^0\pi^0)$ above 700 MeV and $B(\phi \rightarrow \gamma\pi^0\eta)$ are close to the experimental data.

We point out that the branching fraction $B(\phi \rightarrow \gamma f_0)$ is strongly model-dependent, though $B(\phi \rightarrow \gamma\pi^0\pi^0)$ integrated over a mass range given by different experimental groups are mutually consistent within errors as shown in Table 3. The SND collaboration assumes that the whole mass distribution is dominantly given by the $f_0(980)$ resonance with $m_{f_0} = 969.8 \pm 4.5$ MeV and $\Gamma_{f_0 \rightarrow \pi\pi} \approx 200$ MeV, and gives $B(\phi \rightarrow \gamma f_0) = (3.5 \pm 0.3^{+1.3}_{-0.5}) \times 10^{-4}$ [57]. The CMD-2 collaboration gives $B(\phi \rightarrow \gamma f_0(980)) = (3.05 \pm 0.25 \pm 0.72) \times 10^{-4}$ under the single $f_0(980)$ fit, but $(1.5 \pm 0.5) \times 10^{-4}$ under the two-resonance fit with $f_0(980)$ and $f_0(1200)$ [56]. On the other hand KLOE collaboration fits the $\pi^0\pi^0$ mass distribution

in terms of the $\gamma(f_0 + \sigma(600))$ mode with $m_\sigma = 478$ MeV and $\Gamma_\sigma = 324$ MeV, which are obtained in [87], and gives $B(\phi \rightarrow \gamma f_0) = 3 \times (1.49 \pm 0.07) \times 10^{-4} \cong 4.47 \times 10^{-4}$ [58, 60]. In this analysis the σ contribution gives a bump near 500 MeV, but the experimental mass distribution is very small there, so that the bump is erased by the destructive interference with the f_0 resonance with a large width, where $m_{f_0} = 973$ MeV and $\Gamma(f_0 \rightarrow \pi\pi) = 260$ MeV. This enlarges the γf_0 branching fraction. It is further pointed out that their amplitude violates unitarity[15]. We note that a careful analysis using K-matrix parametrization of D_s^+ and D^+ decays into three pions does not need such a low mass σ pole in T-matrix[88].

In theoretical estimates performed by adjusting model parameters so as to fit the experimental data, the branching fraction over the whole mass range is almost consistent with each other. But theoretical estimates of $B(\phi \rightarrow \gamma f_0)$ seem to be model-dependent similarly to the experimental estimates. Our integrated pole contribution $B(\phi \rightarrow \gamma f_0) = 1.97 \times 10^{-4}$ is much larger than the value $0.31 \sim 0.34 \times 10^{-4}$ estimated through calculating pole residues[15], but smaller than the value $3.11 \sim 3.19 \times 10^{-4}$ obtained by integrating $\text{Im}T_{22}$ so as to estimate the f_0 pole contribution [8]. Thus, the branching fraction of the "pure" f_0 signal has not yet been established in theoretical works originating mainly from uncertainties of the parametrization of scattering amplitudes. On the other hand our result $B(\phi \rightarrow \gamma a_0) = 0.7 \times 10^{-4}$ is similar to values of other models.

Unfortunately, it is difficult to deduce a concrete result on the f_0 state from two-photon production processes, because the processes are not dominated by a single production mechanism, and the large charged pion exchange and ω exchange terms mask the f_0 signal originated from the charged kaon loop. Similar complex situation is seen in the $J/\psi \rightarrow \omega f_0$ process. We have observed that mass spectra calculated by the pure pole terms, expressed by appropriate Breit-Wigner forms, are different from those calculated by full scattering amplitudes. This implies that the background coming from the σ enhancement cannot be discarded in comparing calculated results with experimental data.

It is impossible to conclude the quark contents of the light scalar mesons even if we succeed in describing scattering and production processes simultaneously in terms of the OOP amplitudes. We have proposed to study how scattering amplitudes behave as N_c increases from 3, because ChPT is an effective theory of QCD and has the explicit N_c dependence. As a result we have obtained the probable conclusion that while the light vector mesons are of typical $q\bar{q}$ mesons, all of the light scalar mesons below 1 GeV cannot survive as narrow resonances when N_c increases from 3, and then the light scalar mesons cannot be of simple $q\bar{q}$ states.

If the mesons in the light scalar nonet are dominantly composed of hadronic or four quark component, but include $|q\bar{q}\rangle_P$ with a small fraction as in Ref. [1], we could find out the small $|q\bar{q}\rangle_P$ component by increasing N_c in theoretical models, because the large hadronic or four quark component fades out[84] and the $q\bar{q}$ component remains. At least, our calculation within the two-channel OOP approximation does not indicate that such an intriguing change will occur in larger N_c region.

Our conclusion strongly indicates that all of the light scalar mesons are dynamical effects originating from unitarity, chiral symmetry and channel couplings.

A Isospin decomposition of scattering amplitudes and $\omega\pi^0\pi^0$ loop integral

Here we summarize the isospin decomposition of amplitudes written in terms of charged states.

$$\begin{aligned}
\langle \pi^+ \pi^- | T | \pi^+ \pi^- \rangle &= \frac{2}{3} T_{11}^0 + \frac{1}{3} T^2, \\
\langle \pi^+ \pi^- | T | \pi^0 \pi^0 \rangle &= \frac{\sqrt{2}}{3} (T_{11}^0 - T^2), \\
\langle \pi^0 \pi^0 | T | \pi^0 \pi^0 \rangle &= \frac{1}{3} T_{11}^0 + \frac{2}{3} T^2, \\
\langle K^+ K^- | T | \pi^+ \pi^- \rangle &= \frac{1}{\sqrt{3}} T_{12}^0, \\
\langle K^+ K^- | T | \pi^0 \pi^0 \rangle &= \frac{1}{\sqrt{6}} T_{12}^0,
\end{aligned}$$

$$\begin{aligned}
\langle K^+ K^- | T | \pi^0 \eta \rangle &= \frac{1}{2} T_{12}^1, \\
\langle K^+ K^- | T | K^0 \bar{K}^0 \rangle &= \frac{1}{2} (T_{22}^0 - T_{22}^1).
\end{aligned}$$

These amplitudes satisfy unitarity relations from each other.

The $\omega \pi^0 \pi^0$ triangle loop function is given in Appendix B of Ref. [64], which is rewritten so as to fit our normalization and sign.

$$\begin{aligned}
G_3(s) &= \frac{R_\omega}{\sqrt{2}(4\pi)^2} \left\{ 2M_\omega^2 \tilde{L}_2 + s\sigma_1(s) \log\left(\frac{\sigma_1(s) + 1}{\sigma_1(s) - 1}\right) \right. \\
&\quad \left. - s \left(\frac{M_\omega^2 - 2m_\pi^2}{M_\omega^2 - m_\pi^2} + \left(\frac{M_\omega^2}{M_\omega^2 - m_\pi^2} \right)^2 \log \frac{M_\omega^2}{m_\pi^2} \right) \right\}, \\
\tilde{L}_2 &= -Sp(1+iu) - Sp(1-iu) - Sp\left(-\frac{1+\sigma_1}{v}\right) - Sp\left(-\frac{1-\sigma_1}{v}\right) \\
&\quad - \log\left(1 + \frac{1+\sigma_1}{v}\right) \log\left(\frac{1+\sigma_1}{v}\right) - \log\left(1 + \frac{1-\sigma_1}{v}\right) \log\left(\frac{1-\sigma_1}{v}\right) \\
&\quad - \frac{\pi^2}{3} + \pi \tan^{-1} u + i \frac{\pi}{2} \log\left(\frac{1+v+\sigma_1}{1+v-\sigma_1}\right) \quad \text{for } s > 2m_\pi^2, \\
v &= \frac{2(M_\omega^2 - m_\pi^2)}{s}, \\
u &= \frac{\sqrt{s}M_\omega^2}{M_\omega^2 - m_\pi^2},
\end{aligned}$$

where $Sp(z)$ is the double polylog function defined as

$$Sp(z) = - \int_0^z dx \frac{\log(1-x)}{x}.$$

References

- [1] F.E. Close, Summary talk at Hadrom03, hep-ph/0311087.
- [2] , W. Ochs, Talk at Hadron03, hep-ph/0311144.
- [3] N.N. Achasov and V.N. Ivanchenko, Nucl. Phys. B **315** (1989), 465.
- [4] N.N. Achasov and V.V. Gubin, Phys. Rev **D56** (1997), 4084; ibid. D **63** (2001), 094007; ibid. **D64** (2001), 094016.
- [5] F.E. Close, N. Isgur and S. Kumano, Nucl. Phys. **B389** (1993), 513.
- [6] J.A. Oller, Phys. Lett. **B426** (1998), 7.
- [7] E. Marko, S. Hirenzaki, E. Oset and H. Toki, Phys. Lett. **B470** (1999), 20.
- [8] J.A. Oller, Nucl. Phys. **A714** (2003), 161.
- [9] E. Oset, L. Ruca, M.J. Vincent Vacas and J. Palomar, hep-ph/0307037.
- [10] M. Uehara, hep-ph/0206141 (unpublished).
- [11] A. Bramon, R. Escribano, J.L. Lucio M. and M. Napsuciale, Phys. Lett. **B494** (2000), 221.
- [12] A. Bramon, R. Escribano, J.L. Lucio M., M. Napsuciale and G. Pancheri, Eur. Phys. J. **C26** (2002), 253.

- [13] A. Gokalp, A. Küçükarslan, S. Solmaz and O. Yilmaz, J. Phys. **G28** (2002), 2783.
- [14] V.E. Marukushin, Eur. Phys. J. **A8** (2000),389.
- [15] M. Boglione and M.R. Pennington, Eur. Phys. J. **C30** (2003), 503.
- [16] A.V. Anisovich, V.V. Anisovich and V.A. Nikonov, Eur. Phys. J. **A12** (2001),103; A.V. Anisovich, V.V. Anisovich, M.A. Matveev and V.A. Nikonov, Phys. Atom Nucl. **66** (2003),914; A.V. Anisovich, V.V. Anisovich, V.N. Markov, V.A. Nikonov and A.V. Sarantsev, hep-ph/0403123.
- [17] N.N. Achasov and G.N. Shestakov, Z. Phys. **C41** (1988),309.
- [18] K. Hagiwara et al., Phys. Rev. **D66** (2002), 010001.
- [19] J.A. Oller, E. Oset, and J.R. Peláez, Phys. Rev. **D59** (1999), 074001; Erratum Phys. Rev. **D60**(1999), 09906; Phys. Rev. **D62** (2000),114017.
- [20] A.Dobado and J.R. Peláez, Phys. Rev. **D56** (1997), 3057.
- [21] T. Hannah, Phys. Rev. **D54** (1996),4654; ibid **55** (1997), 5613.
- [22] F.Guerrero and J.A. Oller, Nucl. Phys. **B537** (1999), 459; J. A. Oller, Erratum ibid **B602** (2001), 641.
- [23] A. Goméz Nicola and J.R. Peláez, Phys. ReV. **D65** (2002),054009.
- [24] J.R. Peláez and A. Goméz Nicola, AIP Conf. Proc. **660** (2002), 102 [hep-ph/0.01049].
- [25] J. Gasser and H. Leutwyler, Annals Phys. **158** (1984), 142.
- [26] J. Gasser and H. Leutwyler, Nucl. Phys. **B250** (1985), 465.
- [27] J.R. Peláez, Phys. Rev. Lett. **92** (2004),102001: [hep-ph/039292].
- [28] M. Uehara, hep-ph/0308241 (unpublished); hep-ph/0401037 (unpublished).
- [29] J. Weinstein and N. Isgur, Phys. Rev. **D41** (1990), 2236; **D43** (1991), 95
- [30] D. Lohse, J.W. Durso, K. Holinde and J. Speth, Nucl. Phys. **A516** (1990), 513.
- [31] G. Janssen, B.C. Pearce, K. Holinde and J. Speth, Phys. Rev. **D52** (1995), 2690.
- [32] J.A. Oller and E. Oset, Nucl. Phys. **A620** (1997),438; [Erratum; ibid. **A652** (1999), 407].
- [33] M. Uehara, hep-ph/020424 (unpublished).
- [34] P. Estabrooks and A. D. Martin, Nucl. Phys. **B79** (1975), 301.
- [35] G. Grayer et al., Nucl. Phys. **B75** (1974),189: B. Hyams et al., Nucl. Phys. **B64** (1973),134.
- [36] V. Srinivasan et al., Phys. Rev. **D12** (1975), 681.
- [37] L.Rosselet et al., Phys. Rev. **D15** (1977), 574.
- [38] S.D. Protopopescu and A. Alson-Granjost, Phys. Rev. **D7** (1973) 1279.
- [39] D. Cohen et al., Phys. Rev. **D22** (1980), 2595.
- [40] A.D. Martin and E.N. Ozmuth, Nucl. Phys. **B158** (1979), 520.
- [41] W. Hoogland et al., Nucl.Phys. **B126** (1977),109.
- [42] G Colangele, J. Gasser and H. Leutwyler, Nucl. Phys. **B603** (2001),125.
- [43] The KLOE collaboration, hep-ex/0308023.

- [44] J.B. Gay et al., Phys. Lett. **B63** (1976), 220.
- [45] T.A. Armstrong et al., Z. Phys. **C52** (1991), 389.
- [46] J.A. Oller and E. Oset, Phys. Rev. **D60** (1999), 074023.
- [47] V. Bernard, N. Kaiser and Ulf-G. Meissner, Phys. Rev. **D43** (1991), R2757.
- [48] M. Ida, Phys. Rev. **135** (1965), B499.
- [49] J.A. Oller, Nucl. Phys. **A727** (2003), 353.
- [50] S.M. Flattté, Phys. Lett. **63B** (1976), 224.
- [51] R.H. Dalitz and S.F. Tuan, Ann. Phys. **3** (1960), 307.
- [52] J. Nieves and E.R. Arriola, Nucl. Phys. **A679** (2000), 57.
- [53] G. Ecker, J. Gasser, A. Pich and E. de Rafael, Nucl. Phys. **B321** (1989), 311.
- [54] K. Huber and H. Neufeld, Phys. Lett. **B357** (1995), 221.
- [55] A. Bramon, A. Grau and M.R. Pancheri, Phys. Lett **B289** (1992), 97.
- [56] R.R. Akhmetshin et al., Phys. Lett **B462** (1999), 380.
- [57] M.N. Achasov et al., Phys. Lett. **B485** (2000), 349.
- [58] A. Aloisio et al., Phys. Lett. **B537** (2000), 21.
- [59] M.N. Achasov et al., Phys. Lett. **B479** (2000), 53.
- [60] A. Aloisio et al., Phys. Lett. **B536** (2002), 209; N.N. Achasov, hep-ph/0303118. From the latter we read off the data on the mass distribution.
- [61] H. Marsiske et al., Phys. Rev. **D41** (1990), 3324.
- [62] J. Boyer, Phys. Rev. **D42** (1990), 1350.
- [63] H.-J. Behrend et al., Z. Phys. **C56** (1992), 381.
- [64] G. Mennessier, Z. Phys. **C16** (1983), 241.
- [65] J.F. Donoghue, B.R. Holstein and Y.C. Lin, Phys. Rev. **D37** (1988), 2423; J.F. Donoghue and B.R. Holstein, Phys. Rev. **D48** (1993), 137.
- [66] J.A. Oller and E. Oset, Nucl. Phys. **A629** (1998), 739.
- [67] M. Boglione and M.R. Pennington, Eur. Phys. J. **C9** (1999), 11.
- [68] D. Antreayan et al., Phys. Rev. **D33** (1986), 1847.
- [69] T. Oest et al., Z. Phys. **C47** (1990), 343.
- [70] C. Amsler, Rev. Mod. Phys. **70** (1998), 1293.
- [71] G.P. Yost et al., Phys. Lett. **B204** (1988), 1.
- [72] N.N. Achasov, Invited talk at KEK workshop on hadron spectroscopy and chiral particle search in J/ψ data at BES; [hep-ph/0304201].
- [73] A. Falvard et al., Phys. Rev. **D38** (1988), 2706.
- [74] J.E. Augutin et al., Nucl. Phys. **320** (1989), 1.

- [75] M. Uehara, *Prog. Theor. Phys.* **109** (2003), 265.
- [76] E. Witten, *Nucl. Phys.* **B233** (1983), 422, 433.
- [77] G. t'Hooft, *Nucl. Phys.* **B72** (1974), 461; *ibid.* **B75** (1974), 461.
- [78] E. Witten, *Nucl. Phys.* **B160** (1979), 57.
- [79] S. Peris and E. de Rafael, *Phys. Lett.* **B348** (1995), 539.
- [80] P. Herrera-Siklody, J.I. Latorre, P. Pascual and J. Taron, *Nucl. Phys.* **B497** (1997), 345.
- [81] S. Peris, M. Perrottet and E. de Rafael, *JHEP* 9805 (1998), 011.
- [82] M. Harada, F. Sannio and J. Schechter, [hep-ph/0309206](#).
- [83] R.L. Jaffe, *Phys. Rev.* **D15** (1977), 267 and 281.
- [84] R.L. Jaffe, Raporteur's talk at 1981 Lepton-Photon Symposium, Bonn, Germany, Sep. 1981.
- [85] N.N. Achasov, [hep-ph/0309118](#).
- [86] T. Kunihiro, S. Muroya, A. Nakamura, C. Nonaka, M. Sekiguchi and H. Wada, [hep-ph/0310312](#).
- [87] E.M. Aitala et al., *Phys. Rev. Lett.* **86** (2001), 700.
- [88] J.M. Link et al., *Phys. Lett.* **B585** (2004), 200.